

1 **Thermophilic anaerobic digestion of model organic wastes: Evaluation of biomethane**
2 **production and multiple kinetic models analysis**

3 Dinh Duc Nguyen ^{a,b,c}, Byong-Hun Jeon ^d, J. Hoon Jeung^c, Eldon R. Rene^e, J. Rajesh Banu^f,
4 Balasubramani Ravindran^c, Manh Cuong Vu^g, Huu Hao Ngo^h, Wenshan Guo^h, S. Woong Chang^{c,*}

5

6

7 ^a Department for Management of Science and Technology Development, Ton Duc Thang
8 University, Ho Chi Minh City, Vietnam.

9 ^b Faculty of Environment and Labour Safety, Ton Duc Thang University, Ho Chi Minh City,
10 Vietnam.

11 ^c Department of Environmental Energy Engineering, Kyonggi University, Republic of Korea.
12 (nguyendinhduc@tdtu.edu.vn).

13 ^d Department of Earth Resources and Environmental Engineering, Hanyang University, Seoul
14 04763, Republic of Korea.

15 ^e Department of Environmental Engineering and Water Technology, UNESCO-IHE Institute for
16 Water Education, Westvest 7, 2611 AX Delft, The Netherlands.

17 ^f Department of Civil Engineering, Anna University Regional Campus, Tirunelveli Region, Tamil
18 Nadu 627007, India.

19 ^g Center for Advanced Chemistry, Institute of Research and Development, Duy Tan University, Da
20 Nang, Viet Nam.

21 ^h Centre for Technology in Water and Wastewater, School of Civil and Environmental Engineering,
22 University of Technology, Sydney, Australia.

23

24 ***Corresponding author:**

25 E-mail: swchang@kyonggi.ac.kr (S.W. Chang)

26 Abstract

27 The main aim of this work was to test various organic wastes, i.e. from a livestock farm, a
28 cattle slaughterhouse and agricultural waste streams, for its ability to produce methane under
29 thermophilic anaerobic digestion (AD) conditions. The stability of the digestion, potential
30 biomethane production and biomethane production rate for each waste were assessed. The highest
31 methane yield (110.83 mL CH₄/g VS_{added}·day) was found in the AD of crushed animal carcasses on
32 day 4. The experimental results were analyzed using four kinetic models and it was observed that
33 the Cone model described the biomethane yield as well as the methane production rate of each
34 substrate. The results from this study showed the good potential of model organic wastes to produce
35 biomethane.

36 **Keywords:** Organic wastes; biomethane potential; first-order model; modified Gompertz model;
37 Cone model; dual pooled first-order kinetic model.

38 1. Introduction

39 With the growing concern around global warming and in order to confront the persisting
40 global energy crisis, the search for alternative energy resources has been a topic of major concern in
41 the developed and developing nations (Moon et al., 2018). Bioenergy can reduce the demand for
42 fossil energy sources that are depleting at a faster rate (Atelge et al., 2018). Conventional
43 exploitation and use of fossil energy sources contribute to serious environmental problems such as
44 global warming, climate change, and environmental pollution (He et al., 2017; Liu et al., 2015;
45 Whiting and Azapagic, 2014). Anaerobic digestion (AD) has proven to be a sustainable energy
46 producing technology that presents the opportunity and potential for enhancing the reduction,
47 recycling, and recovery of resources from several types of organic wastes (Khalid et al., 2011;
48 Mata-Alvarez et al., 2000; Zou et al., 2016). AD process involves three main phases (including
49 hydrolysis, acidogenesis, and methanogenesis) that require complicated coordination of multiple
50 groups of anaerobic bacteria during each stage. Meanwhile, the quantities and activities of these
51 bacterial groups vary depending on different factors such as the reactors operation conditions,

52 substrate properties and composition, and digester configuration (Yu et al., 2014). The important
53 roles and benefits of AD technology have been widely recognized and applied worldwide. Not only
54 does AD provide beneficial transformation of organic solid wastes into more useful solids (organic
55 amendment), it also produces large amounts of biogas, which is a primary source of sustainable
56 bioenergy (Donoso-Bravo et al., 2011; Ferreira et al., 2013; Nguyen et al., 2016; Romero-Güiza et
57 al., 2016; Yu et al., 2014).

58 Large quantities of organic solid waste are being generated daily from livestock farms,
59 slaughterhouses, and from intense agricultural activities around the world (Liu et al., 2015; Tauseef
60 et al., 2013). Such wastes contain high levels of organic matter that is biodegradable, representing a
61 valuable and economical feedstocks (biomass) for AD (Khalid et al., 2011; Nguyen et al., 2017a;
62 Saxena et al., 2009). The biochemical methane potential (BMP) test is an effective analytical
63 method by which the potential for biological methane production, and the biodegradability of the
64 substrates can be assessed (Kafle and Chen, 2016; Triolo et al., 2011; Triolo et al., 2014). Modeling
65 AD processes can provide optimal solutions for predicting and evaluating the performance of an
66 AD system (El-Mashad, 2013; Yang et al., 2016). Such models can also be used to describe the
67 kinetics of methane production during the AD of different substrates, and can also be helpful for
68 interpreting the effects of changing parameters on the efficiency of the AD system (Xie et al.,
69 2016). The combination of BMP test data and a statistical model can provide substantial benefits in
70 terms of time and cost and can provide an estimation of the optimum design parameters required to
71 support and develop new reactor configurations or to upgrade an existing anaerobic digester (Abudi
72 et al., 2016; Donoso-Bravo et al., 2011; Jurado et al., 2016; Kafle and Chen, 2016; Yang et al.,
73 2016). Several attempts have been made in the literature to describe the dynamics of AD for
74 organic waste treatment (Abudi et al., 2016; Kafle and Chen, 2016; Kouas et al., 2019; Yang et al.,
75 2016; Zhen et al., 2016). However, the models remain underdeveloped because most of the
76 previous studies have focused on the use of a very limited number of substrates and kinetics

77 models, which stimulated the interest of this study in evaluating the utilization of wide range of
78 organic substrates for biomethane production.

79 The main objectives of this study were to: (i) investigate the biomethane production
80 potential from nine different organic waste using a series of batch tests in thermophilic AD, (ii)
81 determine the substrate biodegradable fraction through the measurement and calculation of the
82 elemental composition, and (iii) apply and evaluate four kinetic models, i.e. the Cone model, a first-
83 order kinetic model, the modified Gompertz model, and the dual pooled first-order kinetic model, to
84 describe the kinetics and mechanisms of AD. A comparative evaluation of the four kinetic models
85 was performed to estimate the most suitable one for accurately predicting the biomethane
86 production.

87 **2. Materials and methods**

88 **2.1. Feedstock and inoculum**

89 Different organic wastes were collected from livestock farms, cattle slaughterhouses, and
90 agricultural wastes in various cities of South Korea and ground using a mixer grinder (Dae Sung
91 Artlon Co., Ltd., South Korea), equipped with a fine filtering screen. This process produced a
92 homogeneous mixture with particle sizes < 2.0 mm that was used as the feedstock in the
93 experiments. The characteristics and elemental composition of each type of organic waste are
94 presented in Table 1.

95 **Table 1.** Characteristics of typical organic wastes used in this study.

96 [Insert Table 1]

97 The inoculum for all BMP tests was obtained from a digester using thermophilic anaerobic
98 bacteria to process sewage sludge at the Jinguen biogas plant (Namyangju City, South Korea). The
99 inoculum was sieved through a 1.0 mm mesh and stored in an incubator at 55 °C until further use.
100 Its main characteristics are presented in Table 2. The collection, preservation, and storage of all the
101 samples, including the substrates and the inoculum, followed proper laboratory protocols.

102 **Table 2.** Characteristics of the inoculum used in this study.

103

[Insert Table 2]

104

105 2.2. Practical biochemical methane potential test procedure

106

107

108

109

110

111

112

113

114

115

116

117

118

119

120

121

122

123

124

125

126

127

128

A series of practical biochemical methane potential (PBMP) tests were performed in this study. The batch experiments were carried out for 26 days under conditions that favored thermophilic anaerobes (55 °C). The experiments were performed to determine the potential for methane production from the nine organic wastes, according to previously established protocols (Owen et al., 1979). A PBMP test was conducted for each type of organic waste in 500 mL serum bottles (working volume 300 mL), in which the inoculum size was 20% (v/v), the substrate was 2 g VS/L, and a suitable nutrient medium for the growth and activity of anaerobic microorganisms (Jeong et al., 2019; Nguyen et al., 2017b; Shelton and Tiedje, 1984). The nutrient medium had the following composition: phosphate buffer (to adjust the pH to 7.0 ± 0.1), 270 mg/L KH_2PO_4 , 350 mg/L K_2HPO_4 , mineral salts including 530 mg/L NH_4Cl , 75 mg/L $\text{CaCl}_2 \cdot 2\text{H}_2\text{O}$, 100 mg/L $\text{MgCl}_2 \cdot 6\text{H}_2\text{O}$, and 20 mg/L $\text{FeCl}_2 \cdot 4\text{H}_2\text{O}$, and trace metals including 0.50 mg/L $\text{MnCl}_2 \cdot 4\text{H}_2\text{O}$, 0.05 mg/L H_3BO_3 , 0.05 mg/L ZnCl_2 , and 0.03 mg/L CuCl_2 . The nutrient medium was sterilized in a high-pressure autoclave for ~15 min. The residual oxygen was removed by purging nitrogen gas through a heated (250-300 °C) pipe wound with copper ribbon. To avoid a sudden drop in pH during the acidogenic phase of anaerobic digestion, 1200 mg/L of NaHCO_3 was injected into the medium after it was cooled to 55 °C.

The oxygen remaining in the headspace of all bottles was flushed with nitrogen gas for 3-5 min to create the desired anaerobic condition and avoid aerobic respiration (Koch et al., 2015a).

The bottles were sealed air-tight with screw caps fitted with butyl rubber septa stoppers and were then placed upside down in an incubator in the dark, at 55 ± 2 °C for 26 days. Each digester (bottle) was monitored daily to note the degree of bulging of the rubber septa caused by biogas generation. The biogas pressure generated was controlled, and each bottle was manually shaken, once a day, to mix the contents. Under the same experimental conditions, the control digester containing only the

129 inoculum and the nutrient medium (without substrate added) was also used to determine and correct
130 for methane generated from the inoculum alone.

131 The samples were collected at regular intervals of time until the cumulative biomethane
132 curve almost reached a plateau. The amount of biogas produced in each digester was extracted and
133 measured using a 5 or 10 mL gas-tight syringe until the biogas pressure in the digesters matched the
134 atmospheric pressure. The composition of the biogas collected was analyzed according to
135 previously reported protocols.

136 The volume of biomethane produced during two consecutive measurements, $t-1$ and t , was
137 calculated as follows (Eq. 1) (El-Mashad, 2013):

$$V_{C,t}^{CH_4}(55^\circ C) = C_{C,t} \times V_{G,t} + V_{head} \times (C_{C,t} - C_{C,t-1}) \quad \text{Eq. 1}$$

where $V_{c,t}$ is the volume of biomethane produced in the time interval between $t-1$ and t (in mL), $C_{c,t}$
and $C_{c,t-1}$ are the biomethane concentrations measured at t and $t-1$, respectively, by gas
chromatography (%). $V_{G,t}$ is the volume of biogas produced in the time interval between $t-1$ and t
(%), and V_{head} is the volume of the head space of the digester (mL).

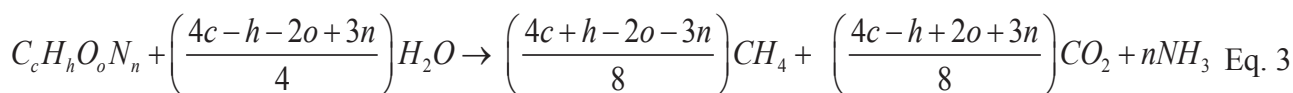
138 The biomethane (CH_4) production (V_{CH_4} , mL) was normalized to volume at standard
139 temperature and pressure conditions (STP: 0 °C and 1 bar) using the ideal gas law (Eq. 2). The
140 specific CH_4 production (mL CH_4 /g VS_{add}) was expressed as the volume of CH_4 produced per g of
141 VS of the substrate added to digesters at the beginning of the BMP tests, as follows:

$$V_{CH_4}(STP) = V_{C,t}^{CH_4}(55^\circ C) \times \frac{(273 K)}{(273K + 55K)} \times \frac{(760mmHg - 118mmHg)}{760mmHg} \quad \text{Eq. 2}$$

The saturated vapor pressure at 55 °C was 118 mm Hg.

142 2.3. Theoretical methane yield and biodegradability calculation

143 The theoretical biochemical methane potential (TBMP) under standard conditions (0 °C, 1
144 bar) was calculated based on the elemental composition of the substrates, according to Buswell's
145 formula (Eqs. 3 and 4):



$$CH_4^{TBMP} \left(\frac{\text{ml } CH_4}{\text{g } VS_{added}} \right) = 22.4 \times \left[\frac{\left(\frac{4c + h - 2o - 3n}{8} \right)}{12c + h + 16o + 14n} \right] \times 1000 \quad \text{Eq. 4}$$

146 The substrate biodegradability was calculated according to Eq. 5 (Browne et al., 2014):

$$\text{Biodegradability (\%)} = \frac{\text{Cumulative methane yield (L / kgVS)}}{\text{Theoretical methane yield (L / kgVS)}} \times 100 \quad \text{Eq. 5}$$

147 The deviation between the experimental values and the simulated values for AD of the
148 substrates was calculated according to Eq. 6:

$$D_{\text{experimental vr. simulated}} (\%) = \frac{|X_{i,\text{Experimental value}} - X_{i,\text{Simulated value}}|}{X_{i,\text{Experimental value}}} \times 100 \quad \text{Eq. 6}$$

149 where D is the deviation between the experimental and the simulated values, $X_{i,\text{experimental}}$ is the
150 experimental value at time i , and $X_{i,\text{simulated}}$ is the simulated value from the model at time i .

151 2.4. Kinetic model analysis

152 A model that was able to describe the complex metabolic processes in the AD and
153 accurately assess the methane yield from the AD of various organic substrates was identified. Four
154 kinetic models including, the Cone model (Eq. 7), a first-order kinetic model (Eq. 8), the modified
155 Gompertz model (Eq. 9), and the dual pooled first-order kinetic model (Eq. 10), were used to fit the
156 cumulative methane production obtained from the experimental data. These models were selected
157 because they have often been used in recent years to describe and predict the kinetics of methane
158 production in AD processes (Brulé et al., 2014; Dennehy et al., 2016; El-Mashad, 2013; Koch and
159 Drewes, 2014; Shin and Song, 1995; Zhao et al., 2018; Zhen et al., 2016; Zhen et al., 2015). The
160 models kinetic parameters were determined and analyzed statistically using Microsoft Excel™
161 2010, with a Solver add-in program (Microsoft, USA) and Origin V8.1 (OriginLab Corporation,
162 USA) *via* non-linear curve fitting of the experimental data. Statistical analyses of the models were
163 evaluated, and the significance was indicated at $p < 0.05$.

Cone model:
$$M(t) = \frac{M_m}{1 + (k \times t)^{-n}} \quad \text{Eq. 7}$$

First-order kinetic model:
$$M(t) = M_m \times (1 - e^{-k \times t}) \quad \text{Eq. 8}$$

Modified Gompertz model:
$$M(t) = M_m \times \exp \left\{ -\exp \left[\frac{R_m \exp(1)}{M_m} (\lambda - t) + 1 \right] \right\} \quad \text{Eq. 9}$$

Dual pooled first-order kinetic mode:
$$M(t) = M_m \times (1 - \alpha \times e^{-k_f t} - (1 - \alpha) \times e^{-k_L t}) \quad \text{Eq. 10}$$

164 where $M(t)$ is the cumulative biomethane production at a given time t (mL CH₄/g VS_{added}),
 165 M_m is the maximum biomethane production potential of the substrate (mL CH₄/g VS_{added}), k is the
 166 hydrolysis rate constant (1/day), t is the time (day), n is the shape factor, R_m is the maximum
 167 specific methane production rate (mL CH₄/g VS_{added}·day), λ is the lag phase time (day), k_f and k_L
 168 are the respective rate constants for a rapidly degradable substrate and slowly degradable substrate,
 169 respectively, and α is the ratio of rapidly degradable substrate to the total degradable substrate.

170 2.5. Analytical methods

171 2.5.1. Sample analysis

172 The volume of biogas production in each digester was measured using a gas-tight syringe at
 173 regular intervals of time. The gas was collected and the methane concentration was measured using
 174 a gas chromatograph (GC) (Agilent 7890A, Agilent Technologies, Inc., USA), equipped with a HP-
 175 PLOT/Q capillary column (split ratio 3:1) (30 m length × 0.53 mm inner diameter, 40 μm film) and
 176 a thermal conductivity detector (GC-TCD). Each sample of biogas (~250 μL) was injected into the
 177 GC with helium as a carrier gas at a flow rate of 30 cm/s. The initial temperature of the GC column
 178 was 60 °C, which was increased to 270 °C at the rate of 30 °C/min. The injector temperature was
 179 set at 230 °C, while the flame ionization detector (FID) was set at 250 °C.

180 The inoculum samples were analyzed for pH, TCOD, SCOD, TS, VS, TN, TAN, FAN, and
 181 Alk. according to the procedure outlined in standard methods (Apha, 2005). The elemental
 182 composition (C, H, N and O) of each substrate was analyzed using an elemental analyzer (Flash
 183 EA1112, CE Instruments, Italy), and the results were reported as percentage of dry weight. Samples

184 were subjected to pyrolysis at high temperature (900 °C), which decomposed them into gases
 185 containing the various elements and allowed measurement of the thermal conductivity of these
 186 gases. The C/N ratio was calculated based on the results of this analysis.

187 2.5.1. Data analysis and model evaluation

188 To determine the best model, the following statistical indicators were determined and
 189 compared: the coefficient of determination (R^2), the F -test, the root mean square prediction error
 190 (rMSPE) (Eq. 11) (Kafle et al., 2013), the second-order Akaike information criterion (AIC) test
 191 (Eq. 12) (Akaike, 1974; El-Mashad, 2013), and the Bayesian information criterion (BIC) test (Eq.
 192 13) (Schwarz, 1978).

$$rMSPE = \left(\frac{1}{m} \sum_{j=1}^m \left(\frac{d_j}{Y_j} \right)^2 \right)^{\frac{1}{2}} = \sqrt{\frac{1}{m} \sum_{j=1}^m \left(\frac{d_j}{Y_j} \right)^2} \quad \text{Eq. 11}$$

where m is number of data pairs, j is the j^{th} value, Y is the measured biomethane production (mL/g
 VS_{added}), and d is the deviation between the experimental and the model fitted methane production.

$$AIC = \begin{cases} N \times \ln \left(\frac{RSS}{N} \right) + 2K, & \text{when } \frac{N}{K} \geq 40 \\ N \times \ln \left(\frac{RSS}{N} \right) + 2K + \frac{2K(K+1)}{N-K-1}, & \text{when } \frac{N}{K} < 40 \end{cases} \quad \text{Eq. 12}$$

$$BIC = N \ln \left(\frac{RSS}{N} \right) + K \ln(N) \quad \text{Eq. 13}$$

where RSS is the residual sum of squares, N is number of data points, and K is the number of model
 parameters.

193 3. Results and discussion

194 3.1. Biomethane generation potential and TBMP of various organic wastes

195 A series of practical biochemical methane potential (PBMP) tests were conducted under
 196 thermophilic conditions. The TBMP for nine different organic substrates was calculated to assess
 197 the overall methane production rates, biomethane yields, and anaerobic biodegradability of the
 198 substrates. As shown in Fig. 1, the daily methane yield (DMY) and cumulative biomethane yield

199 (CMY) were obtained for batch anaerobic digesters after 26 days of operation. The DMY and CMY
200 are the values obtained after subtracting the corresponding biogas yield generated from the control
201 digester. The results of the daily methane yield during the batch anaerobic digestion clearly shows
202 that two peaks appeared for most of the studied substrates (Fig. 1a). The two peaks appeared over a
203 period of 4 to 18 days of digestion, except for OW3, OW5, and OW6 that did not clearly exhibit
204 one or two peaks, due to the biodegradability of the substrates. This mainly depended on the
205 simultaneous processes of hydrolysis and metabolism of accumulated acid and intermediates (e.g.
206 VFAs) (Koch et al., 2015b). The highest daily methane production of all substrates was also
207 observed during this period. There was a gradual decline in the methane production during the end
208 of the experiments, due to the depletion of the substrates. Methane yields were observed in all the
209 digesters, almost instantly after incubation, indicating rapid acclimatization of the anaerobic
210 microbial populations (e.g. methanogenesis) in each digester (Fig. 1a).

211 [Insert Figure 2]

212 **Fig. 1.** Daily methane yield (a) and cumulative biomethane yield (b) from biochemical methane
213 potential tests of various organic substrates during the study period.

214

215 The highest peak of methane yield (110.83 mL CH₄/g VS_{added}·day) was observed using
216 OW3 as the substrate on day 4. However, the highest PBMP was achieved by the OW1 digester
217 (390.05 mL CH₄/g VS_{added}), and it was higher than those obtained from substrates OW2 (5.28%),
218 OW3 (2.01%), OW4 (17.95%), OW5 (55.33%), OW6 (56.87%), OW7 (37.37%), OW8 (10.01%),
219 and OW9 (22.91%) digesters, respectively. Approximately 86-90% of the PBMP after 26 days of
220 digestion was obtained at the end of 21 days for all the substrates studied. This is because of the
221 low substrate concentration available in the digesters after 21 days. The corresponding methane
222 production was very low (0.86 to 5.78 mL CH₄/g VS_{added}·day), depending on the complex organics
223 present in the substrates (Fig. 1b). Compared with the other studied substrates, the PBMP obtained
224 in the OW7, OW6, and OW5 digesters were lowest (244.31, 168.23, and 174.23 mL CH₄/g VS,

225 respectively). This can be attributed to either one of the following reasons: (i) differences in
226 substrate structure and composition (e.g. protein, lignin, and cellulose content) (Koch et al., 2015b),
227 (ii) some portion of the substrate was easily biodegradable as they were already metabolized by the
228 animals digestive systems in the case of OW6 and OW7 (Triolo et al., 2011; Zheng et al., 2015),
229 and (iii) biological conversion processes in the wastewater treatment system for OW5. This would
230 make the remaining portions more difficult or impossible to digest (hydrolyze and biodegrade) by
231 the anaerobic bacteria. In such cases, pretreatment (including chemical, physical, biological, or
232 combinations) of these substrates is essential to enhance anaerobic digestion to simultaneously
233 increase biogas production and reduce the solids content (Nguyen et al., 2017c; Ometto et al.,
234 2014). Detectable biomethane was produced in all the digesters after 12 h of operation, and the
235 CMY increased steadily thereafter irrespective of the type of substrate. This result demonstrates
236 that the digesters were properly prepared (nutrient medium, trace metal, inoculum, and
237 environmental conditions) to enhance the growth of anaerobic bacteria. The theoretical ultimate
238 methane yield of each substrate was calculated (Fig. 2). Using Buswell's equation, the results
239 showed that the yield varied significantly (239.7 to 482.0 mL CH₄/g VS_{added}) depending on the
240 chemical composition of the substrates tested. The highest TBMP value calculated was 482.0 mL
241 CH₄/g VS for OW2, while the lowest value was 239.7 mL CH₄/g VS_{added} for OW6.

242 [Insert Figure 2]

243 **Fig. 2.** Theoretical and experimental biochemical methane potential of various organic substrates
244 during the study period (**a**) and their biodegradability fraction (**b**) (error bars represent 5% of the
245 data).

246 The TBMP values were always higher than the PBMP values for all the substrates tested
247 (Fig. 2a). This is because the TBMPs were calculated based on the chemical composition of both
248 the biodegradable and the non-biodegradable fraction/components of the waste, whereas, only the
249 biodegradable portion was metabolized into biogas through the anaerobic bioconversion process
250 (Kafle and Chen, 2016; Labatut et al., 2011). The anaerobic biodegradability of the substrates was

251 also calculated based on the ratio between the PBMP and the TBMP (Eq. 5) to assess the biological
252 metabolism capacity or methane conversion efficiency of organic substrates under the experimental
253 conditions. The highest biodegradability was 93.04% for OW8, and the lowest was 51.51% for
254 OW5; whereas OW4, OW1, OW3, OW2, OW7, and OW6 were 82.30%, 81.77%, 79.43%, 76.64%,
255 71.62%, and 70.18%, respectively (Fig. 2b). These results clearly indicated that these substrates
256 (except OW5, OW6, and OW7) could be suitable for biodegradation under conditions favoring
257 thermophilic anaerobes, to produce renewable energy and mitigate gaseous emissions. However,
258 pretreatment of OW5, OW6, and OW7 prior to feeding and performing anaerobic digestion was
259 deemed necessary in order to accelerate the anaerobic biodegradability.

260 3.2. Validation and evaluation of the tested kinetic models

261 The selection of an appropriate dynamic model is necessary to simplify and accurately
262 explain the mechanisms and metabolic pathways involved in AD of the substrates under different
263 operating conditions and to predict the performance of individual digesters (Donoso-Bravo et al.,
264 2011; Kafle and Chen, 2016; Prajapati and Singh, 2018). A suitable model is essential for the
265 design, process intensification and long-term AD operation.

266 The experimental data and model predicted curves of cumulative biomethane yield from
267 batch thermophilic AD of nine organic substrates are shown in Fig. 2. The kinetic parameters of the
268 models used to describe the rates of substrate degradation and biomethane production were
269 determined by fitting the experimental data (see Supplementary material). According to the results
270 shown in Fig. 2 and Supplementary material, all the tested models provided reasonable fit to the
271 experimental data. This was confirmed by the high values of determination coefficients (R^2), which
272 were all >0.97 . This indicates that the models employed could explain $>97\%$ of the variations in the
273 results. However, the dual pooled first-order kinetic model was only found to be satisfactory for the
274 substrates OW2, OW3, OW5, and OW9. It appears that the dual pooled first-order kinetic model is
275 probably less flexible and diverse than the other models presented in this work for predicting
276 biomethane production under the study conditions. Hence, it was ascertained that the three other

277 proposed models (Cone model, First-order kinetic model, and Modified Gompertz model) are
278 appropriate for describing the biomethane yield as a function of residence time for the substrates
279 tested in this study. However, each model has its own distinct advantages. For example, the Cone
280 model provides more information on the shape factor, whereas the Gompertz model provides
281 information on the lag phase and the maximum specific methane production rate.

282 The relationship of CMY as a function of AD time with different organic substrates was
283 described by the polynomial regression models (Fig. 3). The relationship was characterized by three
284 main phases: (i) a lag phase (one or two days) in which methane production was detected; however,
285 still at low intensity, (ii) a logarithmic phase during which CMY increased steeply from 2 to 21
286 days due to the rapid growth of the anaerobic bacterial populations, and (iii) the stationary and
287 death phase (after 21 days) wherein the CMY tended to slowly increase until the CMY curve
288 reached a plateau. This plateau may be due to the depletion of the substrate and cell death, owing to
289 which the biomethane production almost ceased.

290 [Insert Figure 3]

291 **Fig. 3.** Experimental data (symbols) and model simulation/prediction (lines) of cumulative
292 biomethane yield from different organic substrates.

293 The hydrolysis rate constant (k) of the substrates determined from the Cone model varied in
294 the range 0.091-0.233 (L/day), which was 25.17-45.07% higher than those obtained from the first-
295 order model. This finding is in accordance to the values reported by Zhao et al. (2016), wherein the
296 value of the hydrolysis rate constant obtained from the Cone model was higher than those obtained
297 using the first-order model. The hydrolysis rate constant varied between substrates, probably due to
298 differences in the composition and structure of the substrate. The results also showed that a lower
299 hydrolysis rate constant was correlated with the decreased biodegradability and longer degradation
300 times required for methane production to reach its maximum value. This observation is also
301 consistent with previously published works (Koch et al., 2015b).

302 The deviation (absolute value) between the experimental CMY and simulated CMY in this
303 study was found to be within the range 0.27-6.07% for the Cone model, 0.13-7.69% for the first-
304 order model, and 1.18-14.03% for the modified Gompertz model, respectively. This reconfirmed
305 the fact that, all the three models can be used for estimating the biomethane potential of these
306 substrates in AD.

307 The maximum predicted methane potential (Mm) of the substrates was estimated from the
308 tested models, which varied depending on the substrates and the model parameter. The Mm
309 predicted by the Modified Gompertz model, first-order model, and Cone model, were always
310 slightly lower than the values obtained from TBMP calculations and were in the ranges of 0.13-
311 0.51%, 0.00-0.45%, and 0.00-0.41%, respectively (Fig. 4).

312 [Insert Figure 4]

313 **Fig. 4.** Comparison of maximum biomethane production potential obtained by different model
314 simulations and by theoretical calculations.

315 3.3. Comparison of proposed models and model selection

316 For practical applications, a model that can predict and evaluate the biomethane production
317 exactly and provide the parameters necessary for optimal design and operation of the AD process of
318 various substrates will save considerable time and operational costs and improve waste
319 management strategies (Mata-Alvarez et al., 2000). Conversely, a wrong choice or inadequate
320 evaluation of the suitability of the model could have many consequences such as incorrect design
321 and operation, resulting in project failure or the inability to meet project requirements (Zhen et al.,
322 2015).

323 The criteria parameters of χ^2 , rMSPE, RSS, AIC, and BIC were calculated (Table 3) and
324 used as the main discriminators to determine a better fit of the model to the experimental data. The
325 lower values of χ^2 , rMSPE, RSS, AIC, and BIC indicate a more appropriate model (El-Mashad,
326 2013; Yang et al., 2016; Zhen et al., 2015). The Cone model had the lowest of rMSPE, RSS, AIC,
327 and BIC, followed in ascending order by the first-order model, the modified Gompertz model, and

328 the dual pooled first-order model. Hence, it is clearly evident that the Cone model exhibited the best
329 biomethane yield fit for the experimental data ($R^2 > 0.985$), and similar observation was also made
330 by other researchers (El-Mashad, 2013; Zhen et al., 2016; Zhen et al., 2015).

331

332 **Table 3.** Criteria for analysis of the best fit of the models to the experimental data.

333

[Insert Table 3]

334

335 When comparing the values for methane yield derived from the Buswell's equation, the
336 model prediction using the best model (Cone), and the experimental results are shown in Fig. 5.
337 After 26 days of anaerobic digestion, the CMYs of substrates OW1-OW9 obtained from the Cone
338 model prediction was compared to the experimental values (in parentheses), as follows: 399.9
339 (390.1), 378.0 (369.4), 383.2 (382.2), 318.6 (320.0), 173.0 (174.2), 158.0 (168.2), 248.5 (244.3),
340 341.2 (351.0), and 304.2 (300.7) mL CH₄/g VS_{added}. This comparison illustrates the deviation
341 between the experimental and predicted values for the different substrates, which were relatively
342 small (2.52%, 2.33%, 0.27%, 0.45%, 0.71%, 6.07%, 1.70%, 2.78%, and 1.16%, respectively). The
343 experimental biomethane production values obtained after 26 days of AD of these substrates was
344 2.02-24.98% which is lower than the maximum biomethane production potential values (Mm)
345 estimated from the Cone model, depending on their degradation rates. This observation clearly
346 indicates that most of the biomethane produced was achieved within 26 days by the utilization of
347 the different substrates by the anaerobic microbial consortia.

347

[Insert Figure 5]

348 **Fig. 5.** Comparison of biomethane production potential obtained by Buswell's calculation: Cone
349 model prediction and experimental results (error bars represent 5% of the data).

350 4. Conclusions

351

352 The measured biomethane yields from thermophilic AD tests, predictions from kinetic
353 models, and theoretical calculations of nine substrates were ascertained in this study. About 86 to
354 90% of the maximal biomethane yield of the substrates was achieved within 21 days. Among the

354 different kinetic models tested, the Cone model fitted the experimental data well and described the
355 kinetics of AD. For practical applications, the Cone model can be used to predict the biomethane
356 production potential of organic substrates, as well as optimize process parameters to enhance the
357 design and operation of an AD process.

358 Acknowledgements

359 This project was supported by grants from the Korean Ministry of the Environment, as a "Global Top
360 Project" (Project No.: 2016002200005), and by the New and Renewable Energy Core Technology Program of
361 the Korea Institute of Energy Technology Evaluation and Planning (KETEP) granted financial resources from
362 the Ministry of Trade, Industry and Energy, Republic of Korea (Project No.: 20143030101040). ERR thanks
363 UNESCO-IHE (Delft) for providing infrastructural and networking support to collaborate with researchers from
364 Republic of Korea.

365 References

- 366 1. Abudi, Z.N., Hu, Z., Sun, N., Xiao, B., Rajaa, N., Liu, C., Guo, D. 2016. Batch anaerobic co-
367 digestion of OFMSW (organic fraction of municipal solid waste), TWAS (thickened waste
368 activated sludge) and RS (rice straw): Influence of TWAS and RS pretreatment and mixing ratio.
369 Energy, 107, 131-140.
- 370 2. Akaike, H. 1974. A new look at the statistical model identification. IEEE Transactions on
371 Automatic Control, 19(6), 716-723.
- 372 3. APHA., WEF. 2005. Standard Methods for the Examination of Water and Wastewater. 21st
373 Edition, American Public Health Association, American Water Works Association and Water
374 Environmental Federation, Washington DC.
- 375 4. Atelge, M.R., Krisa, D., Kumar, G., Eskicioglu, C., Nguyen, D.D., Chang, S.W., Atabani, A.E.,
376 Al-Muhtaseb, A.H., Unalan, S. 2018. Biogas production from organic waste: recent progress and
377 perspectives. Waste and Biomass Valorization (In Press). [https://doi.org/10.1007/s12649-018-](https://doi.org/10.1007/s12649-018-00546-0)
378 00546-0
- 379 5. Browne, J.D., Allen, E., Murphy, J.D. 2014. Assessing the variability in biomethane production
380 from the organic fraction of municipal solid waste in batch and continuous operation. Applied
381 Energy, 128, 307-314.
- 382 6. Brulé, M., Oechsner, H., Jungbluth, T. 2014. Exponential model describing methane production
383 kinetics in batch anaerobic digestion: a tool for evaluation of biochemical methane potential
384 assays. Bioprocess and Biosystems Engineering, 37(9), 1759-1770.
- 385 7. Dennehy, C., Lawlor, P.G., Croize, T., Jiang, Y., Morrison, L., Gardiner, G.E., Zhan, X. 2016.
386 Synergism and effect of high initial volatile fatty acid concentrations during food waste and pig
387 manure anaerobic co-digestion. Waste Management, 56, 173-180.
- 388 8. Donoso-Bravo, A., Mailier, J., Martin, C., Rodríguez, J., Aceves-Lara, C.A., Wouwer, A.V. 2011.
389 Model selection, identification and validation in anaerobic digestion: A review. Water Research,
390 45(17), 5347-5364.
- 391 9. El-Mashad, H.M. 2013. Kinetics of methane production from the codigestion of switchgrass and
392 *Spirulina platensis* algae. Bioresource Technology, 132, 305-312.
- 393 10. Ferreira, L.C., Donoso-Bravo, A., Nilsen, P.J., Fdz-Polanco, F., Pérez-Elvira, S.I. 2013. Influence
394 of thermal pretreatment on the biochemical methane potential of wheat straw. Bioresource
395 Technology, 143, 251-257.

- 396 11. He, S., Fan, X., Luo, S., Katukuri, N.R., Guo, R. 2017. Enhanced the energy outcomes from
397 microalgal biomass by the novel biopretreatment. *Energy Conversion and Management*, 135,
398 291-296.
- 399 12. Jeong, S.Y., Chang, S.W., Ngo, H.H., Guo, W., Nghiem, L.D., Banu, J.R., Jeon, B.-H., Nguyen,
400 D.D. 2019. Influence of thermal hydrolysis pretreatment on physicochemical properties and
401 anaerobic biodegradability of waste activated sludge with different solids content. *Waste*
402 *Management*, 85, 214-221.
- 403 13. Jurado, E., Antonopoulou, G., Lyberatos, G., Gavala, H.N., Skiadas, I.V. 2016. Continuous
404 anaerobic digestion of swine manure: ADM1-based modelling and effect of addition of swine
405 manure fibers pretreated with aqueous ammonia soaking. *Applied Energy*, 172, 190-198.
- 406 14. Kafle, G.K., Chen, L. 2016. Comparison on batch anaerobic digestion of five different livestock
407 manures and prediction of biochemical methane potential (BMP) using different statistical
408 models. *Waste Management*, 48, 492-502.
- 409 15. Kafle, G.K., Kim, S.H., Sung, K.I. 2013. Ensiling of fish industry waste for biogas production: A
410 lab scale evaluation of biochemical methane potential (BMP) and kinetics. *Bioresource*
411 *Technology*, 127, 326-336.
- 412 16. Khalid, A., Arshad, M., Anjum, M., Mahmood, T., Dawson, L. 2011. The anaerobic digestion of
413 solid organic waste. *Waste Management*, 31(8), 1737-1744.
- 414 17. Koch, K., Bajón Fernández, Y., Drewes, J.E. 2015a. Influence of headspace flushing on methane
415 production in biochemical methane potential (BMP) tests. *Bioresource Technology*, 186, 173-
416 178.
- 417 18. Koch, K., Drewes, J.E. 2014. Alternative approach to estimate the hydrolysis rate constant of
418 particulate material from batch data. *Applied Energy*, 120, 11-15.
- 419 19. Koch, K., Helmreich, B., Drewes, J.E. 2015b. Co-digestion of food waste in municipal
420 wastewater treatment plants: Effect of different mixtures on methane yield and hydrolysis rate
421 constant. *Applied Energy*, 137, 250-255.
- 422 20. Kouas, M., Torrijos, M., Sousbie, P., Harmand, J., Sayadi, S. 2019. Modeling the anaerobic co-
423 digestion of solid waste: From batch to semi-continuous simulation. *Bioresource Technology*,
424 274, 33-42.
- 425 21. Labatut, R.A., Angenent, L.T., Scott, N.R. 2011. Biochemical methane potential and
426 biodegradability of complex organic substrates. *Bioresource Technology*, 102(3), 2255-2264.
- 427 22. Liu, L., Zhang, T., Wan, H., Chen, Y., Wang, X., Yang, G., Ren, G. 2015. Anaerobic co-digestion
428 of animal manure and wheat straw for optimized biogas production by the addition of magnetite
429 and zeolite. *Energy Conversion and Management*, 97, 132-139.
- 430 23. Mata-Alvarez, J., Macé, S., Llabrés, P. 2000. Anaerobic digestion of organic solid wastes. An
431 overview of research achievements and perspectives. *Bioresource Technology*, 74(1), 3-16.
- 432 24. Moon, D.H., Lee, S.M., Ahn, J.Y., Nguyen, D.D., Kim, S.S., Chang, S.W. 2018. New Ni-based
433 quaternary disk-shaped catalysts for low-temperature CO₂ methanation: Fabrication,
434 characterization, and performance. *Journal of Environmental Management*, 218, 88-94.
- 435 25. Nguyen, D.D., Chang, S.W., Cha, J.H., Jeong, S.Y., Yoon, Y.S., Lee, S.J., Tran, M.C., Ngo, H.H.
436 2017a. Dry semi-continuous anaerobic digestion of food waste in the mesophilic and thermophilic
437 modes: New aspects of sustainable management and energy recovery in South Korea. *Energy*
438 *Conversion and Management*, 135, 445-452.
- 439 26. Nguyen, D.D., Chang, S.W., Jeong, S.Y., Jeung, J., Kim, S., Guo, W., Ngo, H.H. 2016. Dry
440 thermophilic semi-continuous anaerobic digestion of food waste: Performance evaluation,
441 modified Gompertz model analysis, and energy balance. *Energy Conversion and Management*,
442 128, 203-210.
- 443 27. Nguyen, D.D., Yeop, J.S., Choi, J., Kim, S., Chang, S.W., Jeon, B.-H., Guo, W., Ngo, H.H. 2017b.
444 A new approach for concurrently improving performance of South Korean food waste
445 valorization and renewable energy recovery via dry anaerobic digestion under mesophilic and
446 thermophilic conditions. *Waste Management*, 66, 161-168.

- 447 28. Nguyen, D.D., Yoon, Y.S., Nguyen, N.D., Bach, Q.V., Bui, X.T., Chang, S.W., Le, H.S., Guo,
448 W., Ngo, H.H. 2017c. Enhanced efficiency for better wastewater sludge hydrolysis conversion
449 through ultrasonic hydrolytic pretreatment. *Journal of the Taiwan Institute of Chemical Engineers*,
450 71, 244-252.
- 451 29. Ometto, F., Quiroga, G., Pšenička, P., Whitton, R., Jefferson, B., Villa, R. 2014. Impacts of
452 microalgae pre-treatments for improved anaerobic digestion: Thermal treatment, thermal
453 hydrolysis, ultrasound and enzymatic hydrolysis. *Water Research*, 65, 350-361.
- 454 30. Owen, W.F., Stuckey, D.C., Healy, J.B., Young, L.Y., McCarty, P.L. 1979. Bioassay for
455 monitoring biochemical methane potential and anaerobic toxicity. *Water Research*, 13(6), 485-
456 492.
- 457 31. Prajapati, K.B., Singh, R. 2018. Kinetic modelling of methane production during bio-electrolysis
458 from anaerobic co-digestion of sewage sludge and food waste. *Bioresource Technology*, 263,
459 491-498.
- 460 32. Romero-Güiza, M.S., Vila, J., Mata-Alvarez, J., Chimenos, J.M., Astals, S. 2016. The role of
461 additives on anaerobic digestion: A review. *Renewable and Sustainable Energy Reviews*, 58,
462 1486-1499.
- 463 33. Saxena, R.C., Adhikari, D.K., Goyal, H.B. 2009. Biomass-based energy fuel through biochemical
464 routes: A review. *Renewable and Sustainable Energy Reviews*, 13(1), 167-178.
- 465 34. Schwarz, G. 1978. Estimating the dimension of a model. *The Annals of Statistics*, 6, 461-464.
- 466 35. Shelton, D.R., Tiedje, J.M. 1984. General method for determining anaerobic biodegradation
467 potential. *Applied and Environmental Microbiology*, 47(4), 850-857.
- 468 36. Shin, H.-S., Song, Y.-C. 1995. A model for evaluation of anaerobic degradation characteristics
469 of organic waste: Focusing on kinetics, rate-limiting step. *Environmental Technology*, 16(8), 775-
470 784.
- 471 37. Tauseef, S.M., Premalatha, M., Abbasi, T., Abbasi, S.A. 2013. Methane capture from livestock
472 manure. *Journal of Environmental Management*, 117, 187-207.
- 473 38. Triolo, J.M., Sommer, S.G., Møller, H.B., Weisbjerg, M.R., Jiang, X.Y. 2011. A new algorithm
474 to characterize biodegradability of biomass during anaerobic digestion: Influence of lignin
475 concentration on methane production potential. *Bioresource Technology*, 102(20), 9395-9402.
- 476 39. Triolo, J.M., Ward, A.J., Pedersen, L., Løkke, M.M., Qu, H., Sommer, S.G. 2014. Near infrared
477 reflectance spectroscopy (NIRS) for rapid determination of biochemical methane potential of
478 plant biomass. *Applied Energy*, 116, 52-57.
- 479 40. Whiting, A., Azapagic, A. 2014. Life cycle environmental impacts of generating electricity and
480 heat from biogas produced by anaerobic digestion. *Energy*, 70, 181-193.
- 481 41. Xie, S., Hai, F.I., Zhan, X., Guo, W., Ngo, H.H., Price, W.E., Nghiem, L.D. 2016. Anaerobic co-
482 digestion: A critical review of mathematical modelling for performance optimization.
483 *Bioresource Technology*, 222, 498-512.
- 484 42. Yang, H., Deng, L., Liu, G., Yang, D., Liu, Y., Chen, Z. 2016. A model for methane production
485 in anaerobic digestion of swine wastewater. *Water Research*, 102, 464-474.
- 486 43. Yu, L., Wensel, P.C., Ma, J., Chen, S. 2014. Mathematical modeling in anaerobic digestion (AD).
487 *Journal of Bioremediation & Biodegradation*, S4, 003.
- 488 44. Zhao, C., Mu, H., Zhao, Y., Wang, L., Zuo, B. 2018. Microbial characteristics analysis and kinetic
489 studies on substrate composition to methane after microbial and nutritional regulation of fruit and
490 vegetable wastes anaerobic digestion. *Bioresource Technology*, 249, 315-321.
- 491 45. Zhao, C., Yan, H., Liu, Y., Huang, Y., Zhang, R., Chen, C., Liu, G. 2016. Bio-energy conversion
492 performance, biodegradability, and kinetic analysis of different fruit residues during
493 discontinuous anaerobic digestion. *Waste Management*, 52, 295-301.
- 494 46. Zhen, G., Lu, X., Kobayashi, T., Kumar, G., Xu, K. 2016. Anaerobic co-digestion on improving
495 methane production from mixed microalgae (*Scenedesmus* sp., *Chlorella* sp.) and food waste:
496 Kinetic modeling and synergistic impact evaluation. *Chemical Engineering Journal*, 299, 332-
497 341.

- 498 47. Zhen, G., Lu, X., Kobayashi, T., Li, Y.-Y., Xu, K., Zhao, Y. 2015. Mesophilic anaerobic co-
499 digestion of waste activated sludge and *Egeria densa*: Performance assessment and kinetic
500 analysis. *Applied Energy*, 148, 78-86.
- 501 48. Zheng, Z., Liu, J., Yuan, X., Wang, X., Zhu, W., Yang, F., Cui, Z. 2015. Effect of dairy manure
502 to switchgrass co-digestion ratio on methane production and the bacterial community in batch
503 anaerobic digestion. *Applied Energy*, 151, 249-257.
- 504 49. Zou, S., Wang, X., Chen, Y., Wan, H., Feng, Y. 2016. Enhancement of biogas production in
505 anaerobic co-digestion by ultrasonic pretreatment. *Energy Conversion and Management*, 112,
506 226-235.

507 **Figure captions**

508 Fig. 1. Daily methane yield (a) and cumulative biomethane yield (b) from biochemical methane
509 potential tests of various organic substrates during the study period.

510 Fig. 2. Theoretical and experimental biochemical methane potential of various organic substrates
511 during the study period (a) and their biodegradability fraction (b) (error bars represent 5% of
512 the data).

513 Fig. 3. Experimental data (symbols) and model simulation/prediction (lines) of cumulative
514 biomethane yield from different organic substrates.

515 Fig. 4. Comparison of maximum biomethane production potential obtained from different model
516 simulations and from theoretical calculations.

517 Fig. 5. Comparison of biomethane production potential obtained by Buswell's calculation: Cone
518 model prediction and experimental results (error bars represent 5% of the data).

519

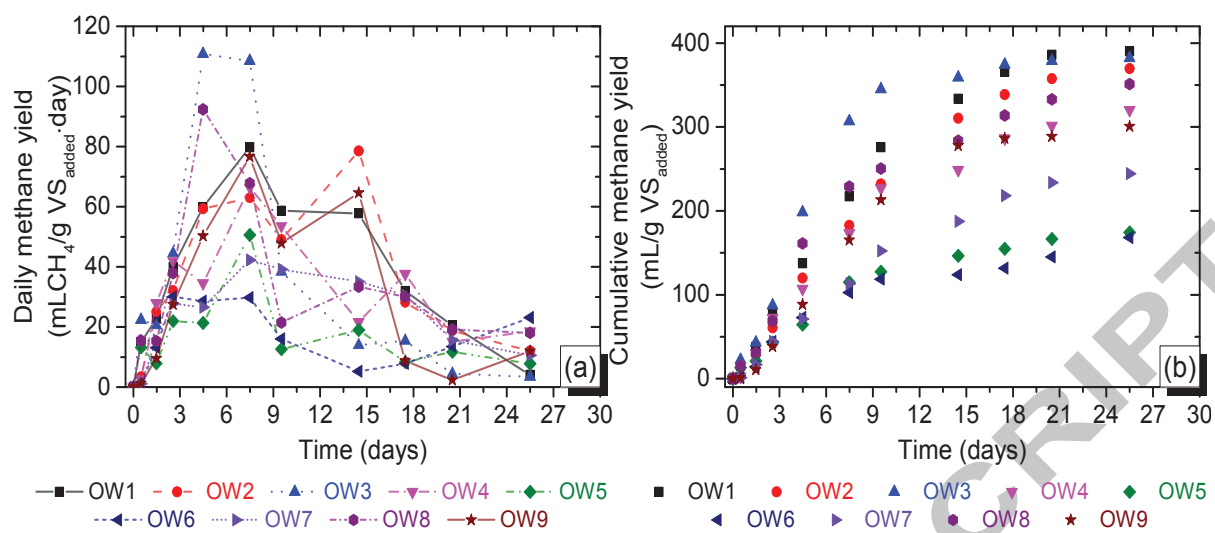


Fig. 1

520

521

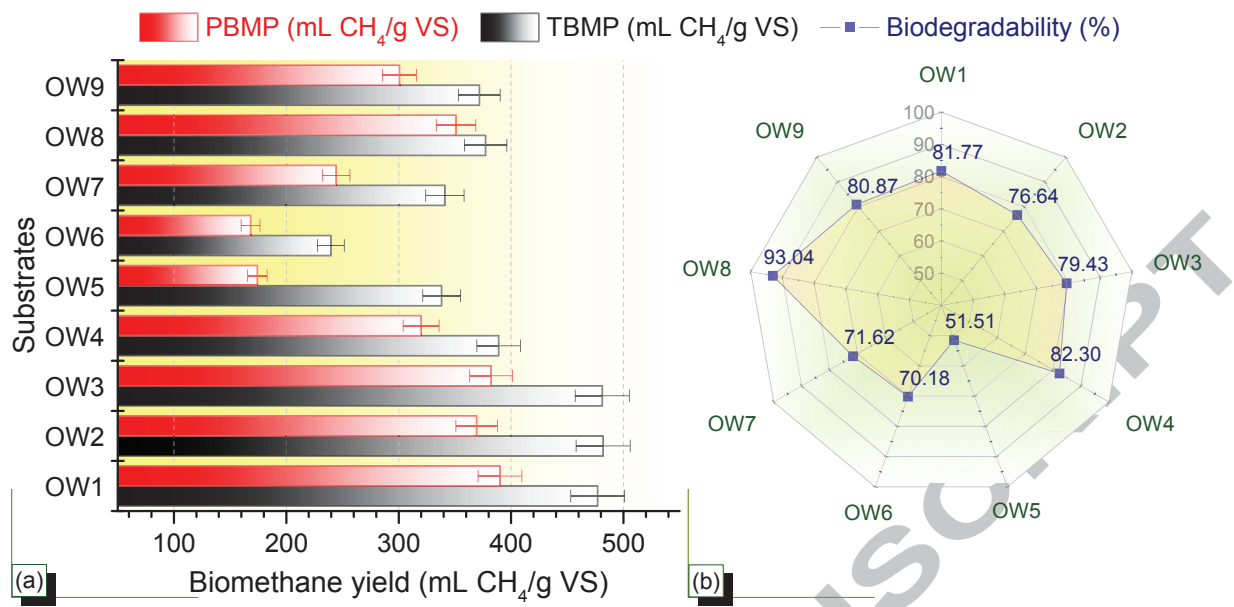


Fig. 2

522

523

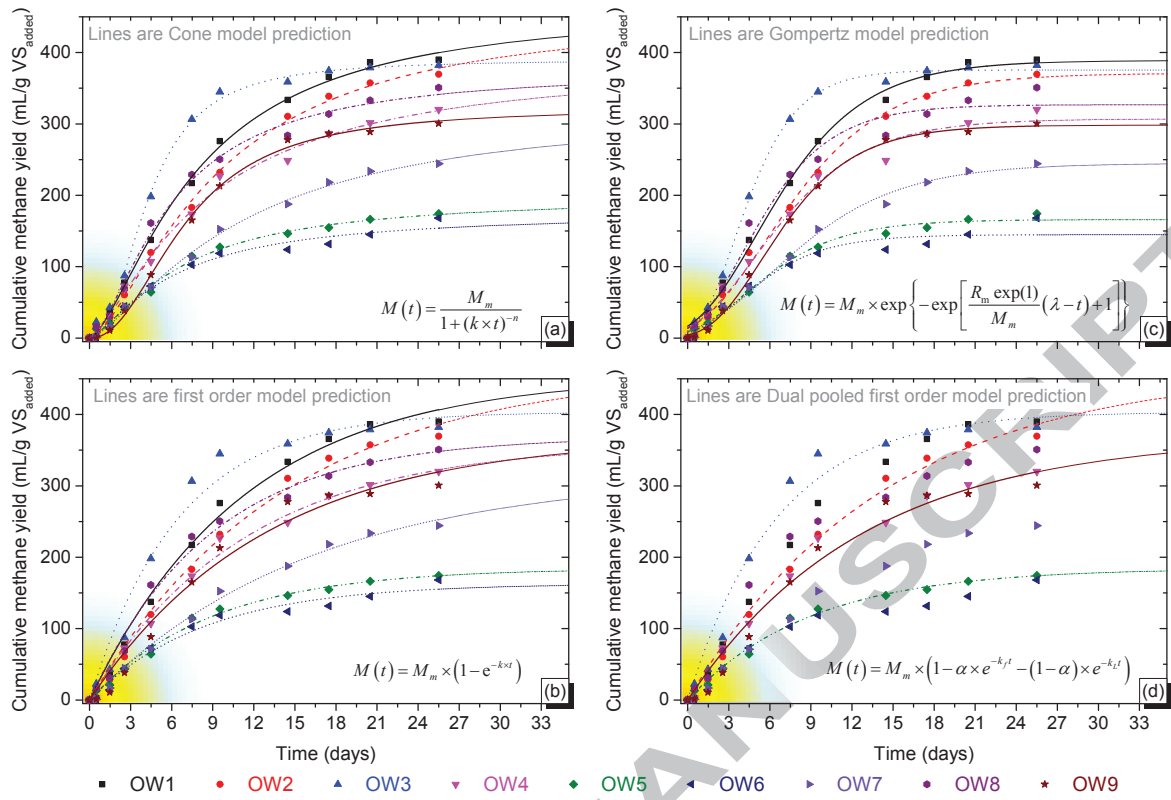


Fig. 3

524

525

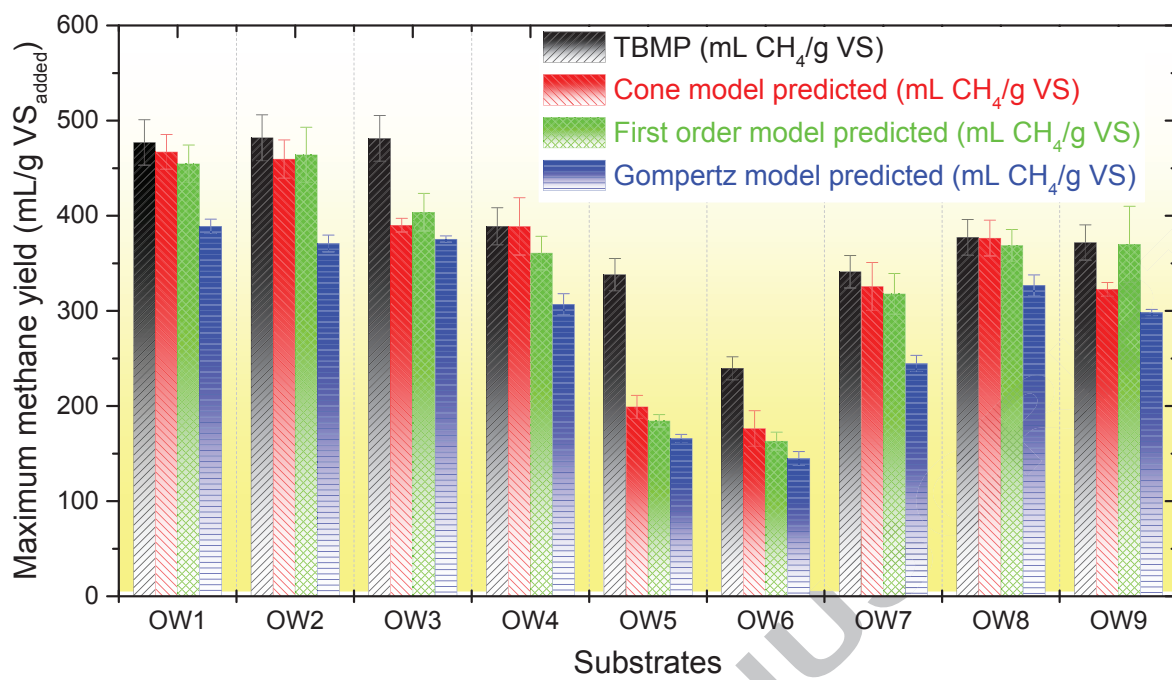


Fig. 4

526

527

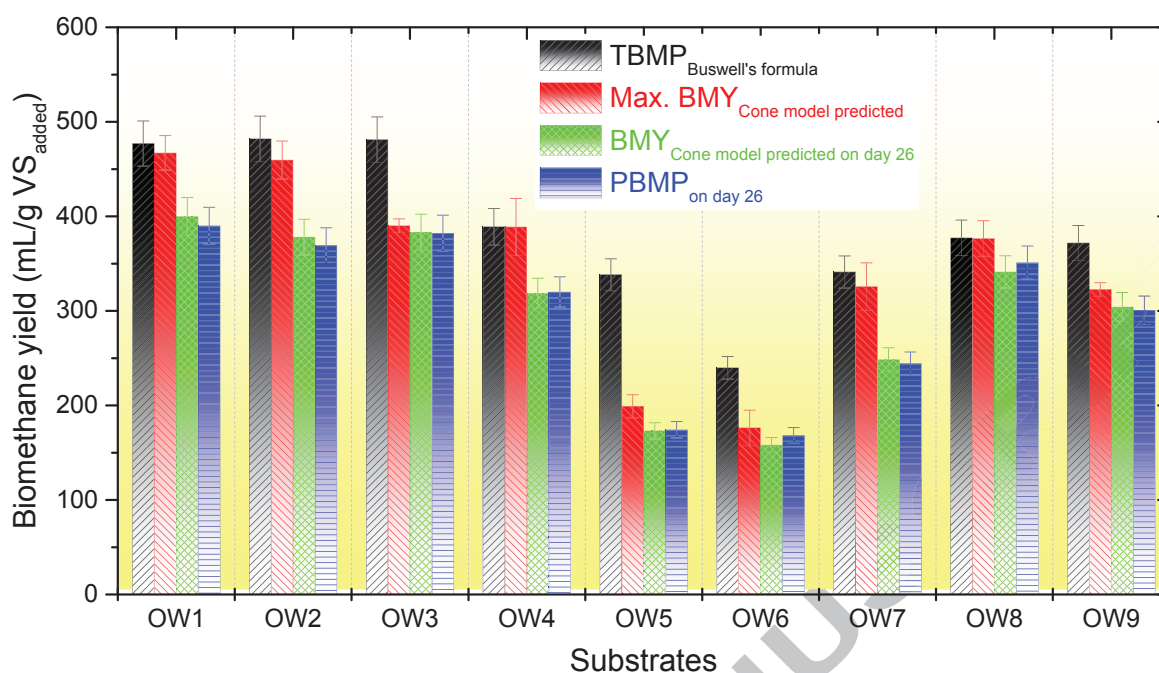


Fig. 5

528

529 50.

530 **Table 1.** Characteristics of typical organic wastes used in this study.

Types of organic wastes	Notation	Elemental composition (% ODM)				C/N ratio	VS (g/L)
		Carbon (C, %)	Hydrogen (H, %)	Oxygen (O, %)	Nitrogen (N, %)		
Pig blood	OW1	64.1	7.3	16.3	10.1	6.35	187.46
Cow rumen (stomach)	OW2	66.0	6.3	25.1	2.5	26.40	214.81
Crushed animal carcasses	OW3	61.9	8.2	19.4	6.4	9.67	327.29
Dehydrated slaughterhouse sludge	OW4	48.1	6.6	20.2	6.6	7.29	116.32
Excess sludge from slaughterhouse WWTP	OW5	45.0	6.1	21.6	7.5	6.00	16.92
Dairy cow manure	OW6	39.3	5.5	31.8	3.5	11.23	176.35
Cattle/animal manure	OW7	43.0	3.6	25.1	2.8	15.36	174.42
Swine manure solids	OW8	49.2	6.5	25.1	3.8	12.95	273.72
Beet leaves	OW9	52.8	6.42	30.17	1.66	31.78	75.97

531

532

533

534 **Table 2.** Characteristics of the inoculum used in this study.

Parameters	Seeding sludge		
	Min.	Max.	Avg. \pm SD
pH	7.83	7.89	7.86 \pm 0.04
Total chemical oxygen demand, TCOD (g/L)	28.04	28.83	28.44 \pm 0.56
Soluble chemical oxygen demand, SCOD (g/L)	2.49	2.55	2.52 \pm 0.04
Total solids, TS (g/L)	25.52	25.80	25.66 \pm 0.20
Volatile solids, VS (g/L)	16.01	16.24	16.12 \pm 0.16
Total nitrogen, TN (g/L)	2.92	3.06	2.99 \pm 0.10
Total ammonia nitrogen, TAN (g/L)	1.16	1.23	1.20 \pm 0.05
Free ammonia nitrogen, FAN (g/L)	0.261	0.275	0.268 \pm 0.01
Volatile fatty acids, VFAs (g/L)	0.06	0.07	0.06 \pm 0.01
Alkalinity, Alk. (g CaCO ₃ /L)	4.02	4.21	4.12 \pm 0.13
VFA/Alk. ratio	0.014	0.016	0.015 \pm 0.001

535

536

537 **Table 3.** Criteria for analysis of the best fit of the models to the experimental data.

Model analysis	RSS	N	Parameter	AIC Test		BIC Test	
				AIC	Akaike weight	BIC	Diff BIC
Cone model	935.609	11	3	63.5	0.855	58.468	0
First-order model	2079.108	11	2	67.0	0.145	64.853	6.386
Modified Gompertz model	2688.253	11	3	75.1	0.017	70.078	5.224
Dual pooled first-order model	2079.108	11	4	79.6	0.0003163	69.649	11.181

538

539 51.

540 **Thermophilic anaerobic digestion of model organic wastes: Evaluation of biomethane**
 541 **production and multiple kinetic models analysis**

542 Dinh Duc Nguyen, Byong-Hun Jeon, J. Hoon Jeung, Eldon R. Rene, J. Rajesh Banu,

543 Balasubramani Ravindran, Cuong Vu Manh, Huu Hao Ngo, Wenshan Guo, S. Woong Chang

544

545 **Graphical abstract**



546

547 52.

548 **Highlights**